Northumbria Research Link

Sessile microdroplet-based writing board for patterning of structural coloured hydrogels

Jing Zhang, Yipeng Qin, Yu Shen, Chao Jiang, You-Tian Tao, Su Chen, Ben Bin Xu and Ziyi Yu*

Dr. J. Zhang, Y. Qin, C. Jiang, Prof. S. Chen, Dr. Z. Yu
State Key Laboratory of Materials-Oriented Chemical Engineering, College of Chemical Engineering, Nanjing Tech University, 30 Puzhu South Road, Nanjing 211816, P. R. China.
Email: ziyi.yu@njtech.edu.cn

Dr. Z. Yu
Department of Chemistry, University of Cambridge, Lensfield Road, Cambridge, CB2 1EW, U.K.

Dr. Y. Shen, Prof. Y. T. Tao
Key Laboratory of Flexible Electronics (KLOFE) & Institute of Advanced Materials (IAM), Jiangsu National Synergetic Innovation Center for Advanced Materials (SICAM), Nanjing Tech University, 30 South Puzhu Road, Nanjing, 211816, P. R. China.

Prof. B. B. Xu
Smart Materials and Surface Lab, Faculty of Engineering and Environment, Northumbria University, Newcastle upon Tyne, NE1 8ST, U.K.

Abstract: The patterning of structural coloured materials has a significant impact on various applications such as flexible displays, anti-counterfeiting patches, colourimetric sensors, *etc*. Herein, a sessile microdroplet-based writing board is presented to pattern magnetochromatic hydrogels with abundant structural colours and improved optical performance. It is demonstrated that predesigned hydrophilic patterns on a hydrophobic writing board can capture a mixture of polymer and $Fe_3O_4@SiO_2$ magnetic nanoparticles inks with a spatial resolution of ca. 100 pin per 1 cm^2 while retaining magnetic field responsibility to the lower limit of 84 Gs. The inks are self-partitioned into microdroplet arrays, which would *in situ* transform into structural coloured hydrogels within a short time *via* thiol-Michael addition. In contrast to conventional evaporation induced assembly of colloidal photonic crystals in sessile droplets, the resulting structural coloured hydrogel microarrays show not only good stability and optical adjustability but tunable morphologies. In addition, the introduction of the microfluidic mixing

and ink dispensing system greatly shortens the time interval from the polymer mixing to sessile droplet generation, circumvents the challenge of short operation time for the self-crosslinking ink components, and enables the direct handwriting of high quality structural coloured patterns.

1. Introduction

The assembly of nano- or microparticles into photonic crystals (PC) that generates structural colours has been the subject of broad research areas to understand their function, structure, performance, and to explore their cutting-edge optical applications. [1, 2] An emerging research paradigm is to develop patterned structural coloured materials capable of dynamic sensing, static identification, or high throughput screening. [3-11] Notable examples include inkjet printing PC arrays with responsive behaviors, [3, 4] spray-coating noniridescent dual-mode coloured PC patterns, [5] direct writing tough rewritable patterned PCs, [6] microfluidic constructing spherical PC arrays, [7-10] and solvent induced preparation of heterogeneous structural colour stripes. [11] These delicate photonic architectures provide inspiring cases for the fabrication of new generation optical devices, expanding a wide range of applications, including sensing, [12, 13] displays, [14, 15] security, [16, 17] and others. [18] However, integrating an easy and low-cost patterning method to the assembled structural colour material is still an open challenge.

Recently, a surface tension-induced sessile microdroplet technique has received considerable attention due to its simple, power-free, and equipment-independent behaviour. [19-21] In this method, non-movable sessile microdroplets are generated in hydrophilic patches of high surface energy compared to the rest of the substrate. By designing the arrays of the hydrophilic areas on the substrate, various microdroplet patterns have been developed in a controllable manner. While extensive studies have focused on applying those microdroplet arrays for high throughput experiments, including cell culture, enzymatic assays, drug screening, and diagnostics, several attempts have been made to illustrate the sessile

microdroplets can also be a powerful alternative to patterning functional materials.[22-25] For example, by using superhydrophobic-superhydrophilic patterned surfaces, Levkin *et al.* demonstrated the generation of hydrogel micropads, [22] the interfacial synthesis of freestanding metal-organic framework microsheets, [23] and the photopolymerization of the poly (ethylenedimethacrylate) microarrays with features down to 30 μm. [24] Song *et al.* pioneered the printing of PC patterns with the aid of hydrophilic/hydrophobic patterned substrates and inkjet printing technology. [25] Because of the asymmetric dewetting of the microdroplet's three-phase contact line, various well-defined structural coloured patterns could be prepared by the assembly of the colloidal particles. However, from the standpoint of the colloidal assembly, there is a need for an improved strategy to generate PC patterns that maintain the high quality of structural colours without the well-known 'coffee-ring' effect. Normally, when colloidal microdroplets form on a substrate, the contact line pinning and faster evaporation rate at the edge of the microdroplets lead to the outward flow of fluid, causing heterogeneously disordered colloidal structures.

In this work, we present the first example of a sessile droplets-based writing board, which enables the construction of customized magnetochromatic patterns with abundant structural colours and improved optical performance. In the presence of an external magnetic field, the magnetic nanoparticles (MNPs) can easily form colloidal strings with tunable interparticle distance, enabling optical modulation in a broad wavelength range that covers the ultraviolet, visible, and infrared light regions. [26, 27] Accordingly, we designed a new type ink of polymer mixtures containing $Fe_3O_4@SiO_2$ MNPs, the colour in which was magnetically tunable when they formed sessile droplets of MNPs-hydrogel composites (**Figure 1A**). This method is not relying on the evaporation-induced assembly of ordered structure to generate colours. Instead, the colour of the patterns is tuned by merely varying the interparticle distance using external magnetic fields. Specifically, the sessile droplets-based writing board was built upon a wettability differentiated substrate along with a continuous ink mixing and supply system.

3

When the inks guided by a writing "pen" rolled across the board surface, they were self-partitioned into microdroplet arrays due to the wettability difference between the hydrophobic and hydrophilic areas of the writing board. Note that the polymers are crucial for this ink microdroplets because further crosslinking of the polymers provides a soft hydrogel matrix to stabilize the dense $Fe_3O_4@SiO_2$ MNPs without precipitation. Importantly, the MNPs maintained external field-response and self-organization capacity behavior. Dynamic optical patterns of various structural colours were built by depositing different colloidal inks in succession, providing an alternative and valuable insight in structural colour patterning.

2. Results & Discussion

2.1 Design of the optical ink.

Herein, the choice of the polymer precursors for the optical ink is based on the following considerations: 1) the polymer precursors are compatible with the MNPs, transform into hydrogels under mild reaction conditions and enable tunable structural colour presentation under external magnetic fields; 2) good biocompatibility, which facilitates their further uses for bio-encoding. From this perspective, commonly used small molecule monomers such as acrylamide are either too toxic or require harsh reaction conditions (either high temperature or ultraviolet radiation). Accordingly, we propose herein an alternative optical ink that could spontaneously change into hydrogels and maintain tunable structural colours upon the application of external magnetic fields. In specific, it contains three parts including the hyperbranched poly (ethylene glycol) diacrylate) (HB-PEGDA) polymer, the thiolated hyaluronic acid (SH-HA) polymer, and $Fe_3O_4@SiO_2$ MNPs. The HB-PEGDA polymer was synthesized *via* the tetraethylthiuram disulfide (DS) mediated reversible addition-fragmentation chain transfer polymerization using excess 2'-azobis (2-methylpronitrile) (AIBN) as the initiator. [28] As **Figure S1** shows, the reaction takes place in several steps. Firstly, the DS reacts with AIBN to form the chain transfer agent DS-AIBN dithiocarbamate *in situ*. Then, the excess
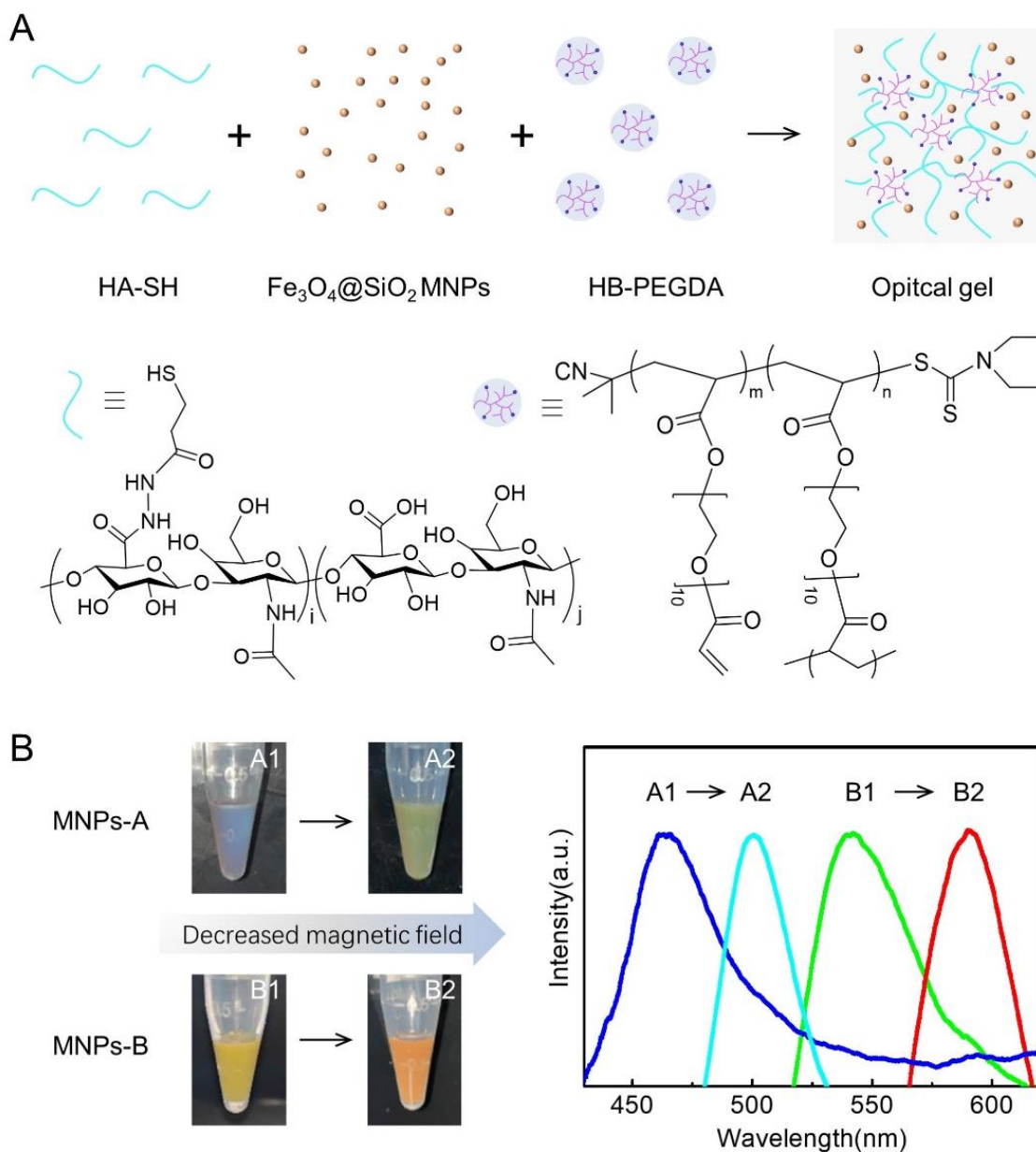
Figure 1 A) Schematic for the preparation of MNPs-hydrogel composites *via* thiol-Michael addition reaction. B) The photograph and reflection spectra of the MNPs-hydrogel composites under external magnetic field. The top two images (A1 and A2) correspond to the sample composed of MNPs with a diameter of 172 nm, and the applied magnetic field strengths (from left to right) are 250 and 120 Gs, respectively. The bottom two images (B1 and B2) are collected from the sample containing MNPs with a diameter of 185 nm, and the applied magnetic field strengths (from left to right) are 300 and 130 Gs, respectively.

AIBN starts to initiate the polymerization of PEGDA in the presence of the already formed DS-AIBN dithiocarbamate. As the reaction proceeds, the polymer molecular weight increases steadily with time (**Figure S2**). When significant levels of the monomer have been consumed,

the conditions of the polymerization were favorable for molecular branching rather than for linear growth, generating hyperbranched HB-PEGDA polymer. When the polymerization was at 30% monomer conversion, the reaction was quenched by opening the flask and exposing the catalyst to air. The chemical structure of the resulting polymer was confirmed by NMR (**Figure S3A**). As a result, the branching ratio of the HB-PEGDA is 45%, indicating 55% of the pendant vinyl ratios remained.

The multiple pendant vinyl groups on the HB-PEGDA polymers could be further crosslinked with SH-HA polymer (**Figure S3B**) to form hydrogels that encapsulate the MNPs *via* thiol- Michael addition under physiological conditions. Briefly, 1.5 % (w/v) HB-PEGDA and 0.2% (w/v) MNPs were vortex mixing with 0.5% (w/v) SH-HA (Mw = 200 - 400 kDa, thiols group contents = 0.68 mmol/g), and its pH value was adjusted to 8.0 using 1 M NaOH solution. Quick gelation was observed within *ca.* 5 min, forming the HB-PEGDA/SH-HA/MNPs hydrogel composites (**Figure S4**). The resulting hydrogel composites are intrinsic brown due to the encapsulated MNPs. When an external magnetic field was applied, they diffracted brilliant structural colour due to the formation of the periodical 1-D chains under balanced interaction of repulsive and attractive forces. [29] In specific, the diffraction wavelength λ could be calculated by using Bragg's equation: [30]

$$\lambda = 2\mathrm{nd}\sin\theta \qquad (1)$$

where λ is the reflection peak position, d is the lattice plane spacing, n is the average refractive index of the optical materials, and θ is the angle between the incident light and lattice planes. Accordingly, when MNPs of smaller size or external magnetic fields with increased intensity are applied, the interparticle spacing d of the MNP chain will decrease and the diffraction peak blue-shifts, demonstrating tunable optical characteristics **(Figure 1B)**.

2.2 Generation of sessile microdroplet arrays with dynamic structural colours

Sessile droplets are adopted here to locally accommodate the aqueous optical ink and generate the microdroplet arrays that compose structural colour patterns (**Figure 2A**). Firstly, a

hydrophilic micropattern was created on a PDMS sheet surface through local oxygen plasma treatment underneath a mask. Due to the wettability difference between the non-treated (hydrophobic) and treated (hydrophilic) areas (**Figure 2B**), the aqueous ink containing HB-PEGDA, SH-HA, and MNPs could readily form an array of sessile droplets on the patterned hydrophilic regions (**Figure 2C**). Then, the self-partitioned droplet microarrays loading with MNPs and polymer precursors *in situ* transform into HB-PEGDA/SH-HA hydrogel composites *via* thiol-Michael addition reaction and give rise to vivid structural colours in the presence of external magnetic fields (**Figure 2D** and **Figure S4**).
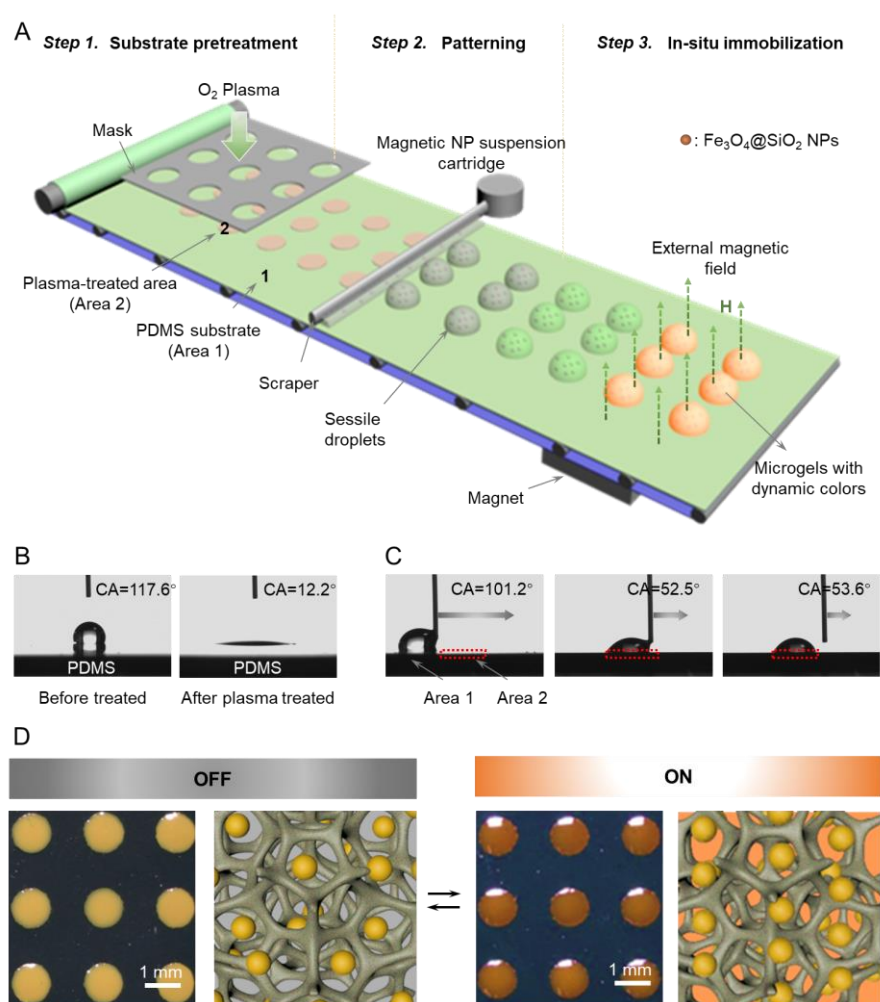
Figure 2 A) Schematic illustration of the preparation process for sessile microdroplet arrays with external magnetic field-response structural colours. B) The contact angle (CA) of the PDMS substrate before and after oxygen plasma treatment. C) Formation of the sessile droplet on the PDMS substrate with hydrophilic dot pattern (marked by the red dotted box). D) The optical images of the resulting sessile droplet arrays before (brown colour, OFF state) and after (red colour, ON state) application of the external magnetic field. MNPs with the size of 185 nm were used.

The *in-situ* formed HB-PEGDA/SH-HA hydrogel greatly enhances the dispersion stability of MNPs in microdroplets, avoiding the particle sedimentation induced by the gravity settling effect. As is well known, the particle distribution in the gravitational field follows:

$$\frac{N_2}{N_1} = \exp\left[-\frac{4}{3}\pi r^3 \left(\rho_{particle} - \rho_{medium}\right)gL\left(x_2 - x_1\right)\frac{1}{RT} \right] \qquad (2)$$

where N_1 and N_2 corresponds to the local number density of particles at height x_1 and x_2, respectively, $\rho_{particle}$ and $\rho_{particle}$ are the density of particles and dispersion medium, r is the particle radius, g is the gravitational acceleration, L is the Avogadro number, R is the molar gas constant, and T is the thermodynamic temperature. Accordingly, the height at which MNP concentration is reduced by half is *ca.* 3 μm at room temperature. Hence, the MNPs in suspensions easily settle at the container bottom under gravity, causing the loss of self-organization capacity and structural colours (**Figure S5**). In contrast, as for the MNPs-hydrogel composites, the MNPs could maintain well dispersed at longer storage time, thus extending their lifetime for structural colour displaying.

While freestanding magnetochromatic beads are used as displaying pixels, [33] they were prepared through the assembly of MNPs inside emulsion droplets and then followed by photopolymerization of the droplets with preserving the ordered structures. However, when these freely moved magnetochromatic beads settle into positioning structures, their rotation caused the angle variation between the incident light and the orientation of 1-D orderly packed MNPs in different beads. This inevitably leads to decreased colour purity, limiting their application in the field of displays, sensors, and pigment fillers (**Figure 3A**). In contrast, the sessile droplet microarrays herein allow consistent orientation of the MNP assemblies under the external magnetic field and thus exhibit uniform colour output (**Figure 3B**). This unique advantage makes the sessile droplet microarrays of great value in the area of displays. Except for the outstanding optical stability and pure colour output, excellent controllability over the
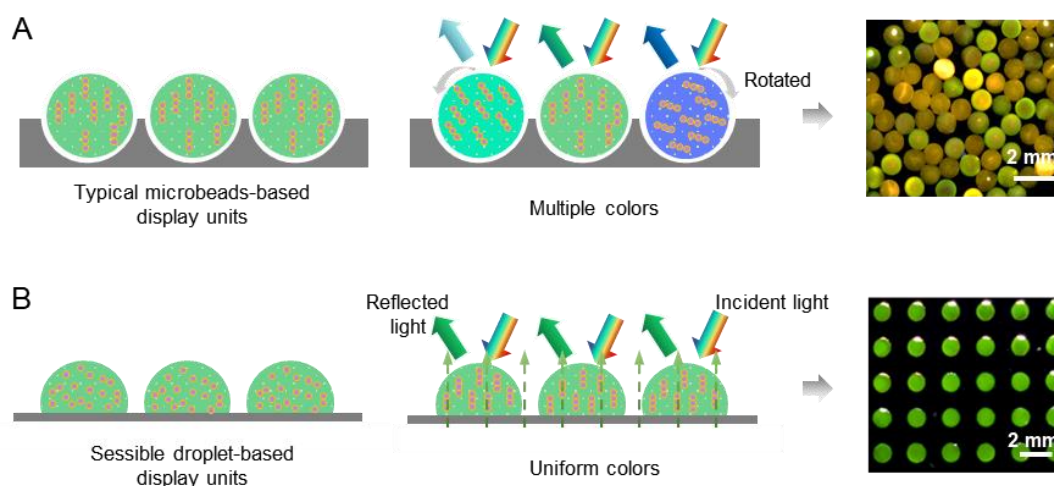
Figure 3 A) The alignment of MNPs in typical freestanding beads and corresponding optical image. B) The alignment of MNPs in sessile microdroplet arrays under external magnetic field and corresponding optical image. The incident light direction is perpendicular to the sample, and MNPs with the same size of 172 nm were used.

morphologies of individual sessile droplets could also be attained. As shown in **Figure 4A** and

Figure 4B, the sessile droplet microarrays in the shape of hemisphere, oval and snowman could

be readily generated by defining the hydrophilic patterns, making it possible to encode extra

information within these individual units, which would be valuable for the high-density bio-

encoding process.

Different from the freestanding magnetochromatic beads that present certain structural

colours due to immobilization of ordered colloid structures in the hydrogel matrixes, [31, 32] the

MNPs-hydrogel composites act more like MNP suspensions. They show natural brown

appearance without an external magnetic field, but the tunable colour appears after the

application of an external magnetic field. To understand this, their microstructures were

investigated by SEM. As **Figure 4C** shows, the HB-PEGDA/SH-HA hydrogel has a macro-

porous structure with pore sizes over 10 μm, and enormous MNPs are noticed attached on the

porous wall surface of the resulting MNPs-hydrogel composites (**Figure 4D**). In addition, the

MNPs exhibit no apparent interaction with the polymer precursors (HB-PEGDA and SH-HA)

(**Figure S6**). Therefore, it can be speculated that the HB-PEGDA/SH-HA hydrogel merely

serves as three-dimensional porous support. The encapsulated MNPs could still move inside the pores and self-assemble into ordered structures under the external magnetic field, exhibiting the characteristic of external field tunable colours. Notably, comparing with conventional magnetic suspensions, the sessile droplets of MNPs-hydrogel composites exhibit a narrower response range indicating a constrained colloidal assembly behavior (**Figure S7**). This could be attributed to that the discrete pores and associated water included confine the magnetic particle locally, thus providing superior dispersion stability but at the same time restricting the movement of the magnetic particles to a certain extent.

Additionally, the *in-situ* formed HB-PEGDA/SH-HA hydrogel also improves the colour stability of the sessile microdroplet arrays under constant external magnetic fields. **Figure S8** shows the reflection spectra variation of the microdroplet arrays that are composed of merely MNP suspension (black line) and HB-PEGDA/SH-HA/MNPs hydrogel composites (red line)
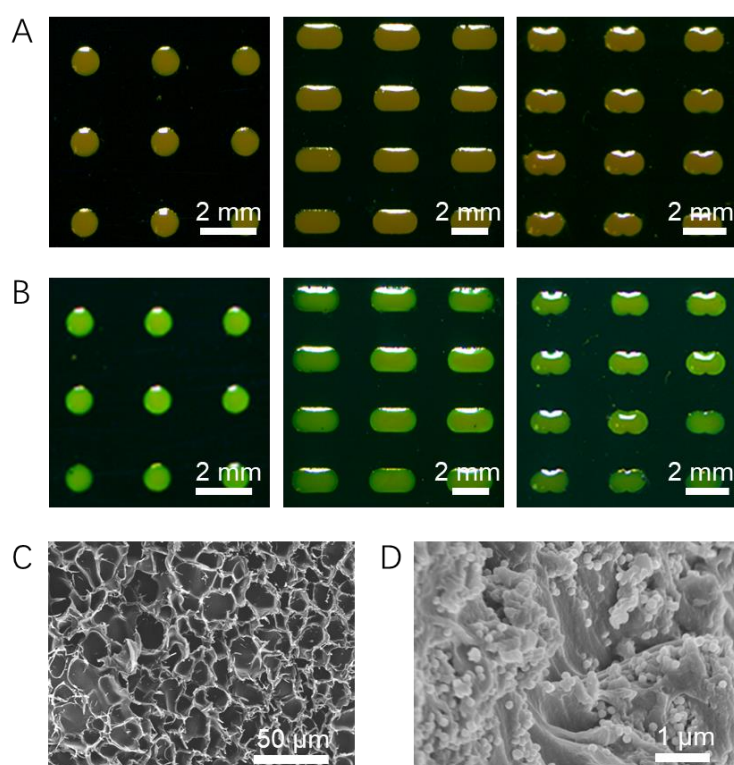

Figure 4 A) Micrograph images of the sessile droplet microarrays with hemispherical, oval, and snowman-like morphologies. MNPs with the size of 172 nm were used. B) The response behavior of the as-obtained sessile microdroplet arrays to the external magnetic field. C) Typical SEM image of the HB-PEGDA/SH-HA hydrogel. D) Typical SEM image of the MNPs-hydrogel composites.

over time under the constant external magnetic field of 150 Gs. The reflection peak intensity of the former dropped rapidly and disappeared within 60 min, while the latter for MNPs-hydrogel composites remained almost unchanged. This phenomenon can be explained by the microcompartment behavior of the HB-PEGDA/SH-HA hydrogel. Furthermore, the gelation process of the HB-PEGDA/SH-HA mixture was studied through oscillation rheology analysis (**Figure S7**). Significantly, the modulus of the gelled mixture is around 10Pa, which gives the hydrogel soft characteristics and facilitates the self-assembly of nanoparticles under a magnetic field. At the same time, the slow gelling behavior of the mixture not only enables rapid extrusion, but also facilitates the uniform dispersion of nanoparticles. As demonstrated above, each micropore of the HB-PEGDA/SH-HA hydrogel serves as a compartment for the MNPs, which prevents the MNPs from sedimentation under the external magnetic field and thus improves the colour stability.

2.3 Sessile microdroplets-based writing board to attain multiple structural coloured patterns

To achieve various structural coloured patterns, we further integrate the sessile droplet technique with a continuous ink mixing and supply system. Specifically, as **Figure 5A** reveals, a hydrophobic substrate with a hydrophilic pattern of densely packed dot arrays (gray area) was prepared as the writing board, while a microfluidic chip with Y-junction geometry was refit into the writing "pen" (the right-most picture of **Figure 5A**). MNPs dispersions containing 3% (w/v) HB-PEGDA at a pH of 9 and aqueous solution containing 1% (w/v) SH-HA at a pH of 7 were introduced separately from the two inlets into the writing pen where they are well mixed before depositing onto the writing board. Then, the mixed ink flows out from the pen tip and be guided by hand rolling across specific regions of the board surface. Once it crosses the hydrophilic dot region, a self-partitioned sessile droplet will be left behind, forming droplet arrays that compose the desired pattern. Through thiol-ene Michael addition of the HB-PEGDA and SH-HA, the as-formed droplets will soon transform into MNPs-hydrogel composites,

exhibiting structural coloured patterns under external magnetic field. It should be noted that this very ink supply system greatly shortens the time interval from the polymer mixing to droplet generation, circumventing the challenge of short operation time for the self-crosslinking ink components. [33] Accordingly, a typical flower pattern was drawn on the board by using optical inks containing two different sized MNPs in succession. As **Figure 5B** shows, all the sessile droplet microarrays show brown appearance without external magnetic field. However, when external magnetic field applies, the leaf area shows saturated green colour, while the petal shows the red colour. To the best of our knowledge, this is the first example of dual structural coloured pattern built upon the sessile droplet technique, and it can reasonably be expected that diverse customizable patterns could be facilely attained when further combining this technique with advanced automatic positioning equipment such as the robot arm.
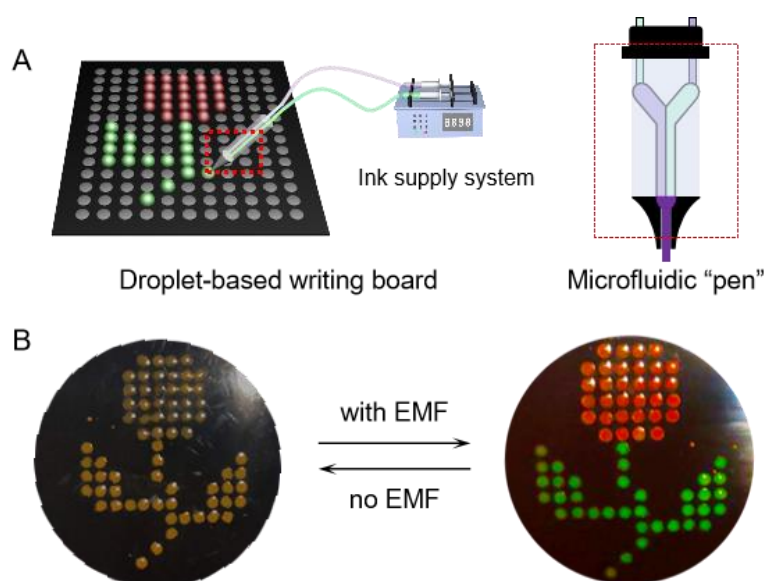
Figure 5 A) Schematic for handwriting of multiply structural coloured patterns by integrating the sessile droplet technique with a continuous ink mixing and supply system. B) Optical image of the resulting flower pattern with dual structural colours.

3. Conclusion

A self-cross-linkable optical "ink" that contains components of HB-PEGDA, SH-HA, and MNPs was proposed in this work. Through thiol-Michael addition polymerization of the HB-PEGDA and SH-HA, the optical ink could spontaneously transform into hydrogels while

maintaining its external magnetic field-response structural colours. Due to the unique support and localisation effect provided by the HB-PEGDA/SH-HA hydrogels, the resulting sessile droplet beads show superior dispersion stability of encapsulated MNPs and present good optical stability. Significantly, the gelation condition of the polymer precursors is very mild and all the optical ink components are biocompatible, facilitating their broad uses in bioencoding and biosensing areas. By further integrating a microfluidic mixing and dispensing system with the sessile droplet technique, a sessile microdroplet-based writing board was constructed, and accordingly direct hand-writing of high quality structural coloured patterns was achieved with sessile droplet arrays. It is reasonable to expect that except for advanced material pattering, this work would also provide valuable insights for areas such as micro liquid handling and micro reactions.

References

[1]   a) Q. Fu, H. Zhu, J. Ge, *Adv. Funct. Mater.* **2018**, *28*, 1804628; b) T. M. Choi, G. H. Lee, Y. -S. Kim, J. -G. Park, H. Hwang, S. -H. Kim, *Adv. Mater.* **2019**, *31*, 1900693; c) P. Wu, J. Wang, L. Jiang, *Mater. Horiz.* **2020**, 7, 338.

[2] a) B. Gao, J. Liao, M. Guo, H. Liu, B. He, Z. Gu, *Adv. Funct. Mater.* **2019**, *29*, 1906745; b) H. Wang, X. Gu, R. Hu, J. W. Y. Lam, D. Zhang, B. Z. Tang, *Chem. Sci.* **2016**, *7*, 5692; c) Y. Takeoka, *Chem. Commun.* **2018**, *54*, 4905.

[3]   a) J. Hou, M. Li, Y. Song, *Angew. Chem. Int. Ed.* **2018**, *57*, 2544; b) J. Zhang, Z. Zhu, Z. Yu, L. Ling, C. -F. Wang, S. Chen, *Mater. Horiz.* **2019**, *6*, 90; c) W. Li, Y. Wang, M. Li, L. P. Garbarini, F. G. Omenetto, *Adv. Mater.* **2019**, *31*, 1901036.

[4]   a) L. Bai, Z. Xie, W. Wang, C. Yuan, Y. Zhao, Z. Mu, Q. Zhong, Z. Gu, *ACS Nano* **2014**, *8*, 11094; b) K. Keller, A. V. Yakovlev, E. V. Grachova, A. V. Vinogradov, *Adv. Funct. Mater.* **2018**, *28*, 1706903.

[5]   Z. Gao, C. Huang , D. Yang, H. Zhang, J. Guo, J. Wei, *Dyes Pigments* **2018**, *148*, 108.

14

[6]   a) X. Su, Y. Jiang, X. Sun, S. Wu, B. Tang, W. Niu, S. Zhang, *Nanoscale* **2017**, *9*, 17877; b) D. Yang, S. Ye, J. Ge, *Chem. Commun.* **2015**, *51*, 16972.

[7]   a) C. Luan, Y. Xu, F. Fu, H. Wang, Q. Xu, B. Chen, Y. Zhao, *Nanoscale* **2017**, *9*, 14111; b) N. Aravindakshan, E. Eftekhari, S. H. Tan, X. Li, J. S. John, N. T. Nguyen, H. Zhao, D. Zhao, Q. Li, *Adv. Optical Mater.* **2020**, *8*, 1901537.

[8]   a) J. Zhang, Z. Meng, J. Liu, S. Chen, Z. Yu, *ACS Appl. Mater. Interfaces* **2019**, *11*, 42629; b) S. -N. Yin, S. Yang, C. -F. Wang, Su Chen, *J. Am. Chem. Soc.* **2016**, *138*, 566.

[9]   a) W. Shen, M. Li, C. Ye, L. Jiang, Y. Song, *Lab Chip.* **2012**, *12*, 3089; b) É. Ruiz-Gutiérrez, J. H. Guan, B. Xu, G. McHale, G. G. Wells, R. Ledesma-Aguilar, *Phys. Rev. Lett.* **2017**, *118*, 218003.

[10]   J. X. Wang, Y. Q. Wen, H. L. Ge, Z. W. Sun, Y. M. Zheng, Y. L. Song, L. Jiang, *Macromol. Chem. Phys*. **2006**, *207*, 596.

[11]   Z. Zhao, H. Wang, L. Shang, Y. Yu, F. Fu, Y. Zhao, Z. Gu, *Adv. Mater.* **2017**, *29*, 1704569.

[12]   a) Q. Xiang, Y. Luo, *Chem. Eng. J.* **2020**, *380*, 122494; b) T. Wang, H. Yang, D. Qi, Z. Liu, P. Cai, H. Zhang, X. Chen, *Small* **2018**, *14*, 1702933; c) F. Qi, Z. Meng, M. Xue, L.Qiu, *Anal Chim Acta* **2020**, *1123*, 91.

[13]   K. R. Phillips, G. T. England, S. Sunny, E. Shirman, T. Shirman, N. Vogel, J. Aizenberg, *Chem. Soc. Rev*. **2016**, *45*, 281.

[14]   a) Y. Wang, W. Li, M. Li, S. Zhao, F. D. Ferrari, M. Liscidini, F. G. Omenetto, *Adv. Mater.* **2019**, *5*, 1805312; b) T. Ding, S. K. Smoukov, J. J. Baumberg, *Nanoscale* **2015**, *7*, 1857; c) A. C. Arsenault, D. P. Puzzo, I. Manners, G. A. Ozin, *Nat. Photon.* **2007**, *1*, 468.

[15]   a) S. Y. Lee, S. H. Kim, H. Hwang, J. Y. Sim, S. M. Yang, *Adv. Mater*. **2014**, *26*, 2391; b) M. Kuang, J. Wang, B. Bao, F. Li, L. Wang, L. Jiang, Y. Song, *Adv. Opt. Mater*. **2014**, *2*, 34.

[16]   a) J. Wang, H. Le-The, L. Shui, J. G. Bomer, M. Jin, G. Zhou, P. Mulvaney, P. W. H. Pinkse, A. Berg, L. I. Segerink, J. C. T. Eijkel, *Adv. Optical Mater.* **2020**, *8*, 1902164; b) Y. Meng, F. Liu, M. M. Umair, B. Ju, S. Zhang, B. Tang, *Adv. Opt. Mater.* **2018**, *6*, 1701351.

[17]   a) J. Hou, H. Zhang, B. Su, M. Li, Q. Yang, L. Jiang, Y. Song, *Chem. Asian J.* **2016**, *11*, 2680; b) Y. Heo, H. Kang, J. S. Lee, Y. K. Oh, S. H. Kim, *Small.* **2016**, *12*, 3819.

[18]   a) J. Zhang, H. Yong, S. A, Q. Xu, Y. Miao, J. Lyu, Y. Gao, M. Zeng, D. Zhou, Z. Yu, H. Tai, W. Wang, *Chem. Mater.* **2018**, *30*, 6091; b) S. Wang, T. Ding, *J. Mater. Chem. C* **2019**, *7*, 13410.

[19]   a) J. Zhang, J. Liu, Z. Yu, S. Chen, O. A. Scherman, C. Abell, *Adv. Funct. Mater.* **2018**, *28*, 1800550; b) T. H. Zhao, R. M. Parker, C. A. Williams, K. T. P. Lim, B. Frka-Petesic, S. Vignolini, *Adv. Funct. Mater.* **2019**, *29*, 1804531; c) H. Lu, Y. Liu, B. B. Xu, D. Hui, Y. Q. Fu, *Compos Part B Eng* **2017**, *122*, 9.

[20]   a) W. Feng, E. Ueda, P. A. Levkin, *Adv. Mater.* **2018**, *30*, 1706111; b) Z. Zhou, J. Zhao, Y. Du, K. Wang, J. Liang, Y. Yan, Y. S. Zhao, *Angew. Chem. Int. Ed.* **2020**, *59*, 1.

[21]   a) L. E. Dodd, D. Wood, N. R. Geraldi, G. G. Wells, G. McHale, B. B. Xu, S. Stuart-Cole, J. Martin, M. I. Newton, *ACS Appl. Mater. Interfaces* **2016**, *8*, 22658; b) X. Cai, N. Xie, Z. Qiu, J. Yang, M. He, K. S. Wong, B. Z. Tang, H. Qiu, *ACS Appl. Mater. Interfaces* **2017**, *9*, 29157; c) Y. Li, P. Chen, Y. Wang, S. Yan, X. Feng, Wei Du, S. A. Koehler, U. Demirci, B. Liu, *Adv. Mater.* **2016**, *28*, 3543.

[22]   A. I. Neto, K. Demir, A. A. Popova, M. B. Oliveira, J. F. Mano, P. A. Levkin, *Adv. Mater.* **2016**, *28*, 7613.

[23]   M. Tsotsalas, H. Maheshwari, S. Schmitt, S. Heißler, W. Feng, P. A. Levkin, *Adv. Mater. Interfaces* **2016**, *3*, 1500392.

[24]   W. Feng, L. Li, X. Du, A. Welle, P. A. Levkin, *Adv. Mater.* **2016**, *28*, 3202.

[25]   a) L. Wu, Z. Dong, M. Kuang, Y. Li, F. Li, L. Jiang, Y. Song, *Adv. Funct. Mater.* **2015**, *25*, 2237; b) H. Li, W. Fang, Z. Zhao, A. Li, Z. Li, M. Li, Q. Li, X. Feng, Y. Song, *Angew. Chem. Int. Ed.* **2020**, *59*,10535.

[26]   M. Wang, L. He, W. Xu, X. Wang, Y. Yin, *Angew. Chem. Int. Ed*. **2015**, *54*, 7077.

[27]   H. Kim, J. Ge, J. Kim, S. Choi, H. Lee, H. Lee, W. Park, Y. Yin, S. Kwon, *Nat. Photonics.* **2009**, *3*, 534.

[28]   D. Zhou, Y. Gao, S. A, Q. Xu, Z. Meng, U. Greiser, W. Wang, *ACS Macro Lett.* **2016**, *5*, 1266.

[29]   a) J. Ge, Y. Hu, Y. Yin, *Angew. Chem.* **2007**, *119*, 7572; b) C. Huang, Y. Cheng, H. Zhang, J. Wei, *Part. Part. Syst. Charact.* **2019**, *36*, 1900238.

[30]   a) W. Wang, X. Fan, F. Li, J. Qiu, M. M. Umair, W. Ren, B. Ju, S. Zhang, B. Tang, *Adv. Optical Mater.* **2018**, *6*, 1701093; b) J. B. Kim, S. Y. Lee, J. M. Lee, S. -H. Kim, *ACS Appl. Mater. Interfaces* **2019**, *11*, 14485.

[31]   a) S. S. Liu, C. -F. Wang, X. -Q. Wang, J. Zhang, Y. Tian, S. -N. Yin, S. Chen, *J. Mater. Chem. C* **2014**, *2*, 9431; b) H. Ma, Y. Tan, J. Cao, S. C. Lian, K. Chen, W. Luo, J. Guan, *J. Mater. Chem. C* **2018**, *6*, 4531.

[32]   J. Ge, H. Lee, L. He, J. Kim, Z. Lu, H. Kim, J. Goebl, S. Kwon, Y. Yin, *J. Am. Chem. Soc.* **2009**, *131*, 15687.

[33]   a) Y. Dong, Y. Qin, M. Dubaa, J. Killion, Y. Gao, T. Zhao, D. Zhou, D. Duscher, L. Geever, G. C. Gurtner, W. Wang, *Polym. Chem.* **2015**, *6*, 6182; b) Z. Q. Liu, Z. Wei, X. L. Zhu, G. Y. Huang, F. Xu, J. H. Yang, Y. Osada, M. Zrínyi, J. H. Li, Y. M. Chen, *Colloids Surf. B* **2015**, *128*, 140.
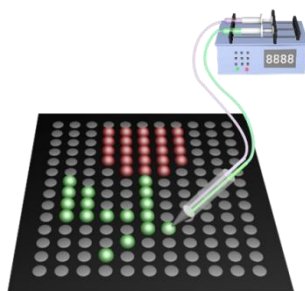
A sessile microdroplets-based writing board is successfully built upon a wettability differentiated substrate along with a continuous ink mixing and supply system, enabling the flexible design of magnetochromatic patterns with abundant structural colours and improved optical performance.

Keyword sessile microdroplets, photonic crystals, patterning, structural colours

Dr. J. Zhang, Y. Qin, Dr. Y. Shen, C. Jiang, Prof. Y. T. Tao, Prof. S. Chen, Prof. B. B. Xu and Dr. Z. Yu*

Sessile microdroplets-based writing board for patterning of structural coloured materials

ToC figure

A sessile droplets-based drawing board
for structural color patterning

Supporting Information

A sessile microdroplet-based writing board for patterning of structural coloured materials

Jing Zhang, Yipeng Qin, Yu Shen, Chao Jiang, You-Tian Tao, Su Chen, Ben Bin Xu and Ziyi Yu*

1. Experimental

1.1 Materials $FeCl_3 \cdot 6H_2O$, $ZnCl_2$, poly(ethylene glycol) diacrylate (PEGDA, average Mn = 575), Dithiothreitol (DTT), tetraethylthiuram disulfide and urea were obtained from Shanghai Aladdin Bio-Chem Technology Co., LTD. Sodium citrate ($C_6H_5O_7Na_3 \cdot 2H_2O$) and polyacrylamide (PAM, Mw = 3000 kDa) were from Sinopharm Chemical Reagent Co., Ltd. 3,3'-Dithiobis(propanoic dihydrazide) (DTP) was obtained from Frontier Scientific Co., LTD. 1-Ethyl-3-(3-dimethylaminopropyl)carbodiimide hydrochloride (EDCI) was purchased from Damas-beta, Shanghai Titan Scientific Co., Ltd. Fermentation-derived hyaluronan (HA, Mw = 200 ~ 400 kDa) was purchased from Bloomage Biotechnology Co., LTD. All other starting chemicals were purchased from Sigma-Aldrich and used as received without further purification, unless stated otherwise. The Y-typed microfluidic chip was designed according to the previously reported method.[1] A Millipore Milli-Q system provided deionized water with a resistance greater than 18 m$\Omega \cdot$cm^{-1}.

1.2 Synthesis of Fe_3O_4@SiO_2 core/shell MNPs. The preparation of Fe_3O_4@SiO_2 core/shell MNPs comprises two steps: 1) hydrothermal synthesis of monodispersed superparamagnetic Fe_3O_4 nanoparticles [2] and 2) the silica coating process. [3] Briefly, to synthesize Fe_3O_4 nanoparticles, 0.17 g of $FeCl_3 \cdot 6H_2O$, 0.01g of $ZnCl_2$, 1.58 g of $C_6H_5O_7Na_3 \cdot 2H_2O$, and 1.44 g

of urea were dissolved in 75 mL of distilled water, and a certain amount of PAM ranging from 0.50 g to 1.00g was added under vigorous stirring for 12 h. The aqueous mixture was then transferred into a 100 mL polytetrafluoroethylene-lined autoclave and heated at 200 ℃ for 10 h. The as-obtained Fe_3O_4 nanoparticles was seperated by centrifugation, washed with deionized water and dried in a vacuum at room temperature. Redisperse the Fe_3O_4 nanoparticles in 3 mL of deionized water for the coating process. The coating of Fe_3O_4 nanoparticles with a thin layer of silica was achieved through a modified Stöber process. Typically, 1.2 mL of ammonia solution (28 wt%) and 5 mL water were first added into the above aqueous suspension of Fe_3O_4 nanoparticles (3 mL) and sonicated for 5 min. 40 mL of absolute ethanol was subsequently added to the solution and further sonicated for another 5 min. The solution was then transferred into a 250mL three-neck flask and 160μL of TEOS was added at once. The reaction continued at room temperature for 2 h under mechanical stirring with a speed of 400 rpm. The resulting $Fe_3O_4@SiO_2$ core/shell MNPs were collected by a magnet, washed several times with deionized water and dried in a vacuum at room temperature.

1.3 Synthesis of HB-PEGDA. The HB-PEGDA polymer was synthesized by an *in-situ* RAFT approach. Briefly, PEGDA monomer (30 mmol, 25 equiv) was first dissolved in 75 mL of butanone at a monomer concentration of 0.4 M in a two-neck flask. Then, the initiator AIBN (1.7 mmol, 1.4 equiv) and tetraethylthiuram disulfide (DS, 1.2 mmol, 1 equiv) were added into the flask. The mixture was bubbled with argon for 30 min. The reaction commenced after heating the mixture to 70 °C. The polymerization was monitored by an Agilent 1260 Infinity GPC system equipped with a refractive index detector, a viscometer detector, and a dual-angle light-scattering detector (LS 15° and LS 90°). GPC columns (PolarGel-M, 7.5×300 mm^2; two in series) were eluted with DMF and 0.1% LiBr at a flow rate of 1 mL/min at 60 °C. GPC columns were calibrated with linear poly(methyl methacrylate) standards. To measure the molecular weight and monomer conversion, GPC samples were collected at regular intervals.

20

The resulting HB-PEGDA products were purified four times by precipitating in excess solvent mixture containing hexane and diethyl ether with a volume ratio of 1:2 and dried at room temperature in a vacuum for 24 h before use. Chemical composition and branching ratio of the HB-PEGDA polymer were further determined with ^{1}H NMR (Bruker, 400 MHz).

1.4 Synthesis of SH-HA. In brief, 500 mg of HA and 2.5 mmol of DTP were first dissolved in 10 mL of MES buffer (0.1M，pH = 4.75). Then, 2.5mmol of EDCI was added into the solution. The pH of the mixture was maintained at 4.75 during the reaction by addition of 1.0 M HCl. After 5 h, the reaction was stopped by addition of 1.0 M NaOH, raising the pH of the reaction mixture to 7.0. 3.25mmol of DTT was subsequently added and the pH of the solution was raised to 8.5 by addition of 1.0 M NaOH. After the mixture was stirred for 24h, the pH of reaction mixture was adjusted to 3.5 by addition of 1.0 M HCl. The acidified solution was then transferred into the dialysis tubing (Mw cutoff = 12 kDa) and dialyzed against dilute HCl (pH=3.5) containing 100 mM NaCl for 24 h, followed by dialysis against dilute HCl (pH = 3.5) for another 24 h. The solution was then centrifuged, and the supernatant was lyophilized. The free thiols on the side chain of SH-HA were determined by a modified Ellman method. [4]

1.5 Preparation of the HB-PEGDA/SH-HA/MNP hydrogel composites *via* thiol-Michael addition reaction.[5] The optical hydrogel composites were fabricated as follows: the HB-PEGDA polymer was dissolved in PBS buffer to a concentration of 3 (w/v)%, and MNPs were added into the solution to a concentration of 0.4 wt%; the SH-HA polymer was diluted with PBS buffer to a concentration of 1 (w/v)% and its pH value was adjusted to 8 using 1 M NaOH solution; then, the two solutions were mixed together with equal volumes by vortex for 5 s to attain the optical hydrogel composites. The reflection spectra of the optical hydrogel composites under external magnetic field were collected by the optic spectrometer (Ocean Optics, USB4000).

21

2. Supplementary Figures

Figure S1 Synthesis of HB-PEGDA *via* the DS mediated reversible addition-fragmentation chain transfer polymerization using excess 2'-azobis (2-methylpronitrile) (AIBN) as the initiator. The RAFT agent was formed *in situ* from the initiator AIBN and the DS.
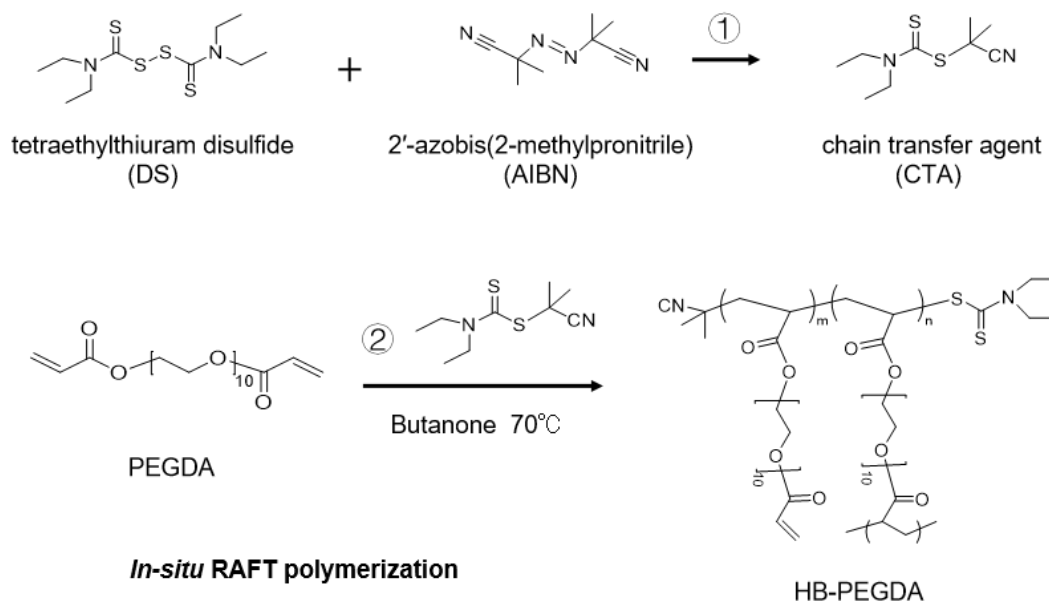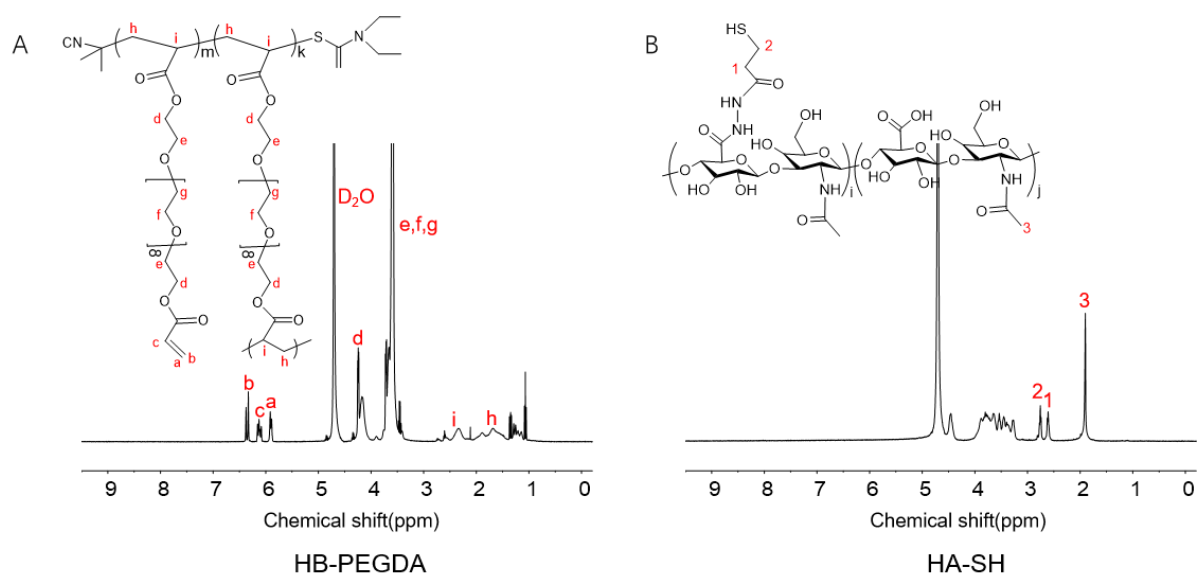
**Figure S2** GPC traces of HB-PEGDA polymers isolated at different reaction time.
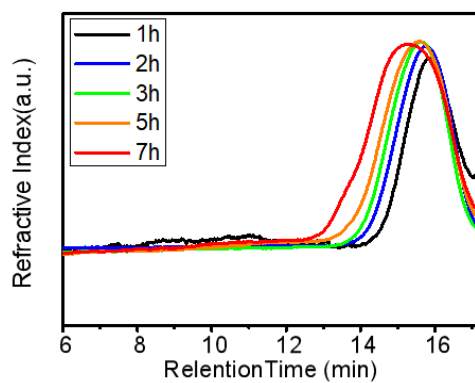
Figure S3 Chemical structure and corresponding ^{1}H NMR spectra of the HB-PEGDA polymer and SH-HA polymer (Mw = 200 - 400 kDa, thiols group contents = 0.68 mmol/g).

Figure S4 Real time rheological measurements of the HB-PEGDA (1.5% w/v)/SH-HA (0.5% w/v) mixture (5% strain, 1Hz). G′ and G″ represent the storage modulus and loss modulus of the forming HB-PEGDA/SH-HA/MNPs hydrogel composites.
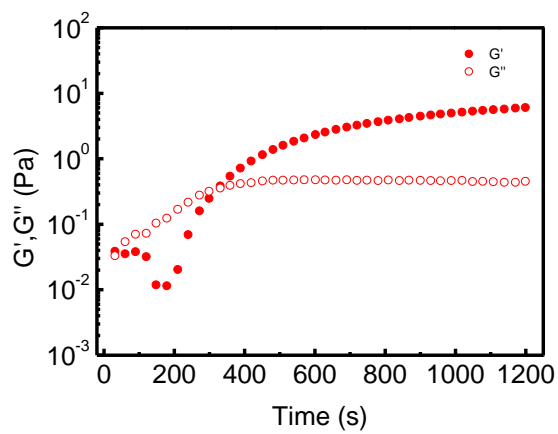
Figure S5 Optical images of the sessile microdroplet arrays in the presence of external magnetic field. Scale bar = 2 mm. The red coloured arrays were composed of MNPs with the size of 185 nm, while the green and blue were composed of MNPs with the same size of 172 nm but they were applied with different strengths of external magnetic fields.
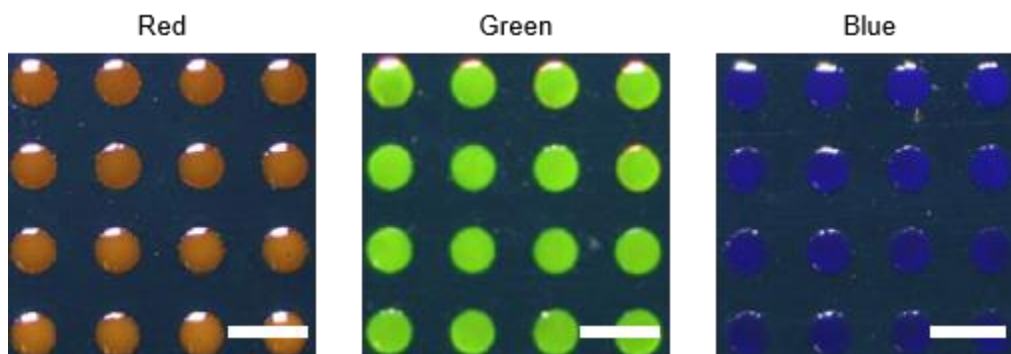
Figure S6 A) From the left to right correspond to the MNP suspension, the MNP suspension containing 1.5% (w/v) HB-PEGDA, the MNP suspension containing 0.5% (w/v) SH-HA and MNPs-hydrogel composite. B) The optical images of the above suspensions after a storage time of 5 h.
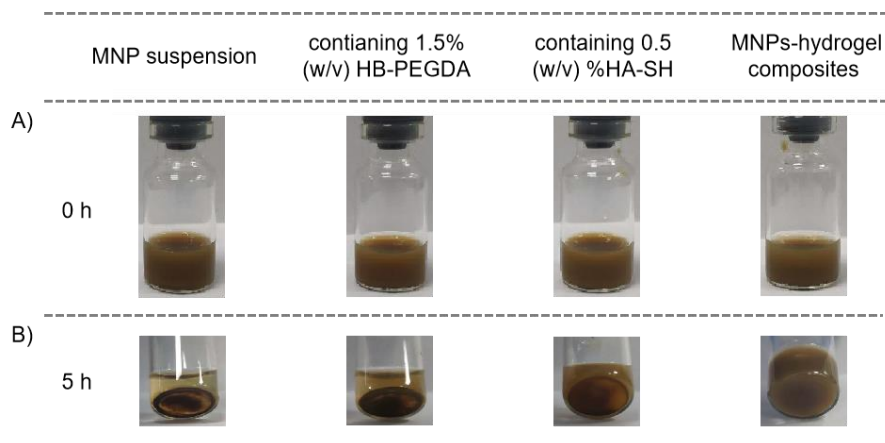
Figure S7 The reflectance spectra of the MNP suspension and the sessile droplets of MNPs-hydrogel composites under magnetic field with different strengths.
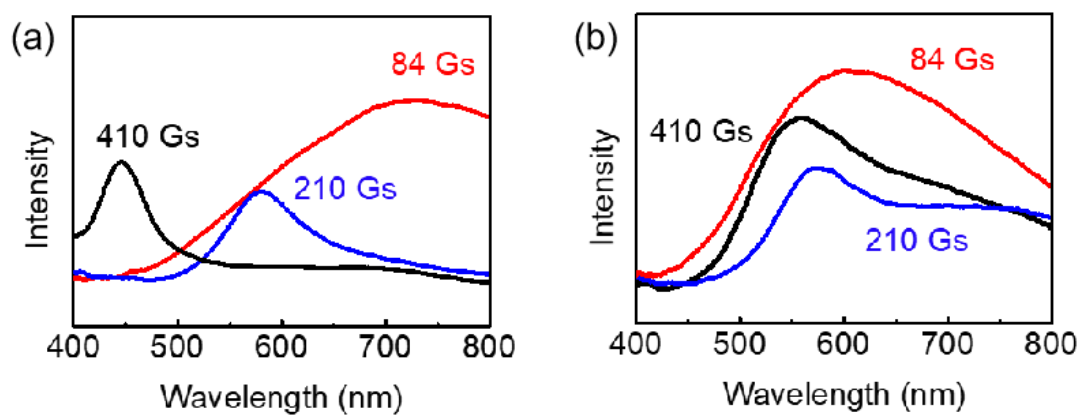
Figure S8 The reflection spectra variation of the MNP aqueous suspension (Black Line) and the hydrogel microarrays (Red Line) over time under a constant external magnetic field of 150 Gs.
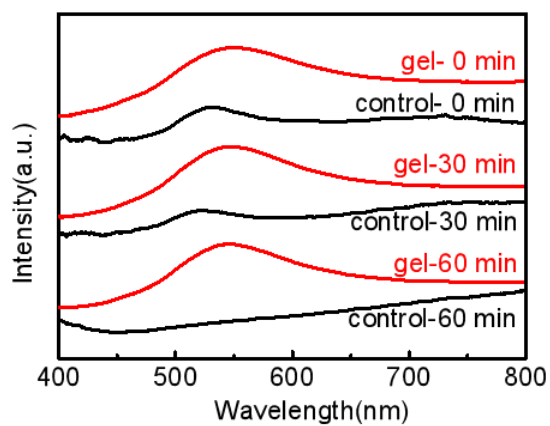
References

[1]   Y. Zheng, Z. Yu, R. M. Parker, Y. Wu, C. Abell, O. A. Scherman, *Nat. Commun.* **2014**, *5*, 5772.

[2]   W. Cheng, K. Tang, J. Sheng, *Chem. Eur. J.* **2010**, *16*, 3608.

[3]   W. Wang, X. Fan, F. Li, J. Qiu, M. M. Umair, W. Ren, B. Ju, S. Zhang, B. Tang, *Adv. Optical Mater.* **2018**, *6*, 1701093.

[4]   X. Z. Shu, Y. Liu, Yi Luo, M. C. Roberts, G. D. Prestwich, *Biomacromolecules* **2002**, *3*, 1304.

[5]   a) Y. Dong, Y. Qin, M. Dubaa, J. Killion, Y. Gao, T. Zhao, D. Zhou, D. Duscher, L. Geever, G. C. Gurtner, W. Wang, *Polym. Chem.* **2015**, *6*, 6182; b) Z. Q. Liu, Z. Wei, X. L. Zhu, G. Y. Huang, F. Xu, J. H. Yang, Y. Osada, M. Zrínyi, J. H. Li, Y. M. Chen, *Colloids Surf. B* **2015**, *128*, 140.